Proceedings World Geothermal Congress 2023

Beijing, China, April 17 – 21, 2023

Radioactive Geochemical Characteristics of a Certain Geothermal Fields In Jizhong Depression, N- China

Gongxin Chen[1,2], Zhanxue Sun[1,2], Han Su[3], Jinhui Liu[1,2], Angdong Wang[1,2], Dexuan Kong[1,2] and Yong Fan[1,2],

1.State Key Laboratory of Nuclear Resources and Environment，East China University of Technology，Nanchang，330013，Jiangxi， China

2.East China University of Technology，Nanchang，330013，Jiangxi， China

3.312000；Shaoxing Water Conservancy Bureau，Shaoxing 312000，China

E-mail address, gxchen@ecit.edu.cn; zhxsun@ecut.edu.cn; Jhliu@ecut.edu.cn; 313226623@qq.com;

Keywords: Geothermal, Thermal Conductivity, Radioactive Geochemical Characteristics, radiogenic heat flux of Rock, Jizhong Depressure.

ABSTRACT

As we all known, geochemical exploration has been widely used in geothermal resource exploration . In recent study, it was found a good potential resource of thermal water for exploration from Jizhong Depression North-east China. In this paper, both of soil geochemical and rock radioactive geochemical characteristics have been studied to provide useful information for the deep geothermal resource exploration in this region. Soil elements, such as *As, Bi, Sb, Hg, Be, As, Li, Cu, Zn, Mn, Co, Cs, Sc, Ni, Pb, Rb, Sn, Mo* and *W*, were significantly self-correlated as thermal fluids up-flowing. These elements were enriched to a certain concentration in some area, in Niutuozhen Uplift in, south of study area. Their abundance were higher than those from Daxing Uplift. Their distribution has a good related to the distribution of deeper and larger faults, such as Daxing and Niudong Fault. High ^{210}Po concentration from soil and high radon from thermal water were occurred in Niutuozhen area in the south area. This abundance of these elements in the soil indicated that the deep hydrothermal fluids flew up along the regional faults. Thermal conductivity of both limestone and dolomite were with average values of 3.92W/mK and 5.75W/mK, respectively. These were higher than those of other type rocks, while, radiogenic heat flux was lower than others rocks, with average values of 0.75 μW/m^3 and 0.19 μW/m^3. This indicated that these two type rocks could contribute of conduct heat flow from the depth to form heat reservoir. The overburden of mud-stone and conglomerate with huge thickness, low water permeability, and low thermal conductivity (2.35W/mK and 3.24W/mK average) were good to keep heat escaping from thermal reservoir. Thermal conductivity of gneiss rock, which found in the depth with 2.59W/mK in average, was lower than those of other rocks, but the radiogenic heat flux , with 1.26μW/m3 in average, was higher than that of other rocks. According to radioactive geochemical characteristics, the percentage of heat flow from crust was calculated ranging from 36.9% to 48.4%, which was less than 50%. This indicated that lithographer thermal structure in these region has a typical "hot mantle cold crust" characteristics. Heat were from mantle through conduction was greater than from crustal radiogenic heat.

0 INTRODUCTION

Geothermal, as a kind of clean energy, has been widely concerned by many scientists and scholars. At present, it has been applied in hot spring development, breeding, heating, power generation, medical treatment and other aspects[1-2]. The annual production of geothermal resources in China was almost equivalent to 70% of coal consumption in 2015, however, the use of geothermal resources in China only accounts for 0.6% of the country's total energy consumption[3] .The Tianjin-Beijing-Hebei region was believed to be one of the most regions in rich geothermal resources, which not only has good geothermal occurrence, but also has large amount of resources and were easy to develop[4].InHebei Province , China, geothermal reserves were as high as 100,549 million tons of standard coal, and the annual utilization of geothermal water was equivalent to 327,000 tons of standard coal, which can reduce CO_2 emissions by about 780,200 tons, SO_2 emissions by about 50,600 tons, and suspended dust by about 2,600 tons[5] .Therefore, geothermal resources utilization has significant benefits for local economic and social development. Jizhong Depression, located in the northern part of the North China Plain, was rich in geothermal resources and has great potential for development. For example, Niutuozhen in Gu 'an, known as "hot spring town", was one of the key areas for geothermal development in the Beijing-Tianjin-Hebei region1 Geological background of the study area[6-8].

As we all known, geochemical exploration has been used in geothermal resource exploration as one of the most effective and economical methods. In this study, the geochemical characteristics of the soil front halo, the characteristics of the shallow geothermal field and the thermal physical properties of rocks were studied in the northern part of Jizhong Depression, aiming to provide basic data for the geothermal exploration in Jizhong Depression.

1GEOLOGICAL SETTING

The study area is located in the northern part of Jizhong Plain, which belongs to the alluvial plain in front of Taihang Mountain and Yanshan Mountain. The terrain was flat, about 100m above sea level, and the terrain gently slopes from northwest to southeast, with l/200 ~ l/2000slope.Water system in the region includes Yongding River in the west, Baigou River in the east, and Beijuma River and Xiaoqing River in the north. Jizhong depression belongs to the North China Basin, which was connected with Taihang Mountain uplift in the west,

Cangxian Uplift and Huanghua Depression in the east .It can be divided into 10 structural units (Fig. 1). This work area covers 6 units of them, namely, Beijing sag, Daxing Uplift, Dachang Sag, Langgu Sag, Niutuozhen Uplift and Baxian Sag.

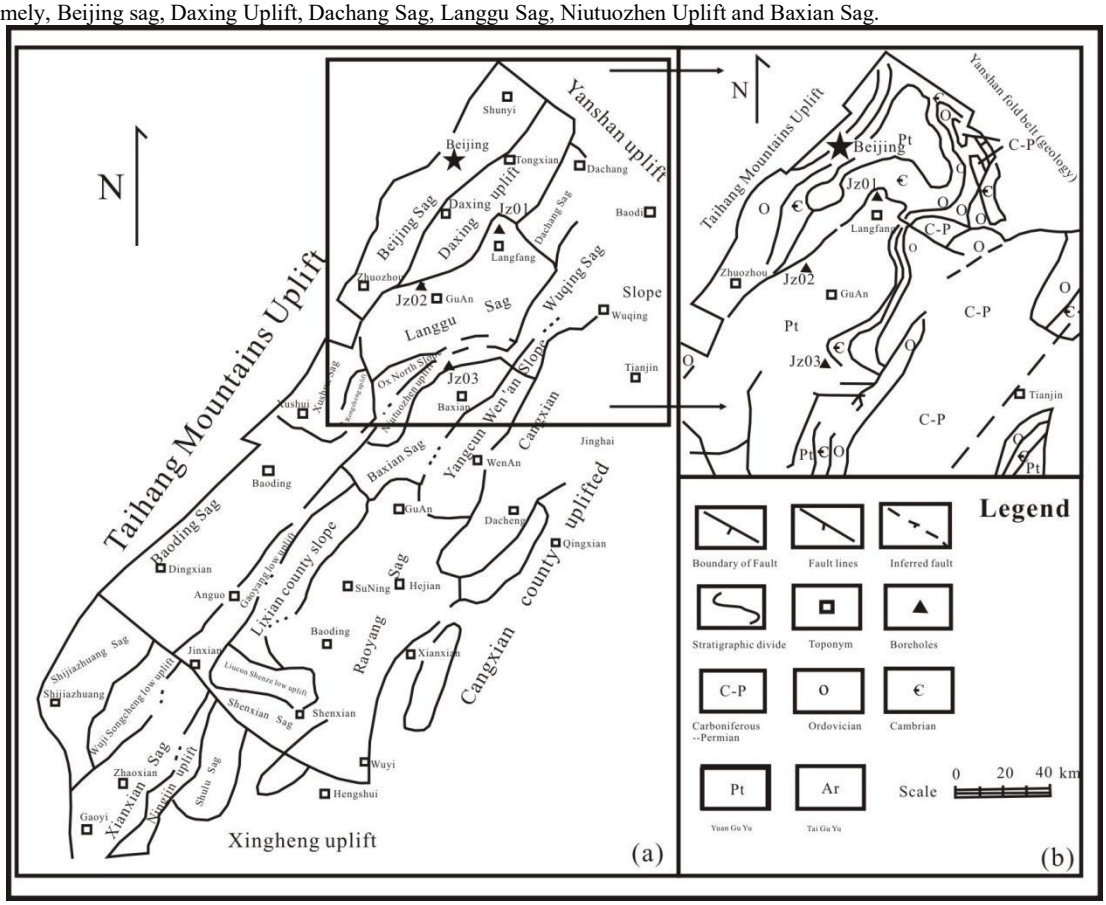

Figure 1 Geological Structure(modified from Du Jinhu et[9],2002)

(a)Geological structure division and (b)underlying characteristics of Mesoproterozoic and NeoProterozoic

2 SAMPLING AND ANALYSIS METHODS

2. 1 soil sampling

GA-I~GA-IX, sampling points were set on the profile to ensure that the soil sample collection density was 1 /km^2(Figure 2). Among them, GA-I~GA-IV is located in the north of the study area. GA-V~GA-IX is located in the south of the study area,the spacing is about 2km, the spacing of sampling points is about 1km, 164 points in total.

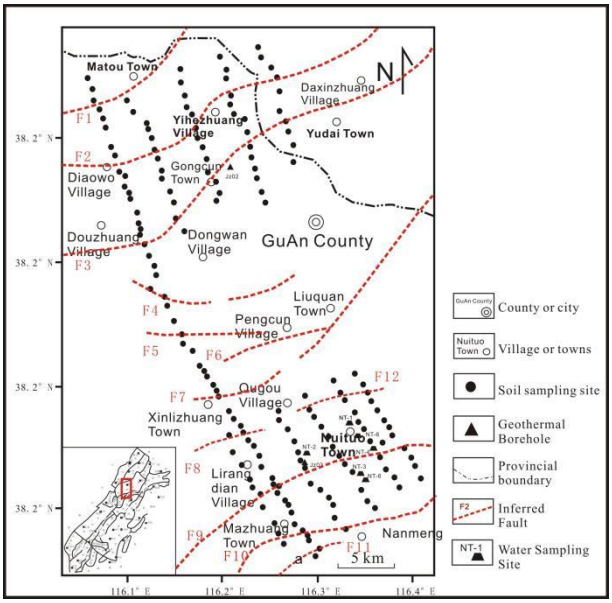

Figure 2 Sampling points in the study area

Due to the limitations of the site and equipment conditions, the Luoyang shovel with a diameter of 5cm was used to manually drill holes in this soil sampling work. The drilling and sampling depth were both 5 meters, and the changes of the surface soil were recorded. The sampling weight was 1kg.

(3)Test instruments and methods

- Hg element: Determination of mercury content by aqua regia atomic fluorescence method.
- As, Sb, Bi, Be, Li and other 14 elements: Determination of super trace elements by inductively coupled plasma mass spectrometry with four-acid digestion method.
- ^{210}Po Element: copper foil self-deposition total α counting method determination of ^{210}Po content .

2.2 rock Sampling

A total of 101 rock samples were collected. Three were collected from outcrop rock in Taihang Mountain other 98 sample from geothermal borehole *JZ01*, *JZ02* and *JZ03* (as shown in Fig. 2.2)., ranging from 200 to 3200 m depth,. Rock density, thermal conductivity, radioactive thermogenic elements *U*, *Th*, *K, were analyzed*. A total of 101 rock samples collected from the field were tested for rock density.The text instrument used was XF-220SD high precision digital display solid and liquid densitometer, with an accuracy of 0.0001g /cm^3. Rock thermal conductivity tests were analyzed by C-Therm TCI thermal conductivity instrument(Canadian C-Therm Company).The accuracy was better than 5%, and the test repeatability was better than 1%. The analysis was conducted at the State Key Laboratory of Nuclear Resources and Environment, East China University of Technology.

3.Result and discussion

3.1 Geochemical characteristics of elements related thermal reservoir

Element correlation analysis were standardized. and R-type cluster analysis was carried out by the SPSS software for *As*, *Be*, *Bi, Li, Cu, Sb, Zn, Hg, Mn, Co, Cs, Sc, Ni, Pb, Rb, Sn, Mo, W, ^{210}Po* and other elements. The R-type cluster analysis result was shown as in mass spectrogram (Fig. 3) . In this figure, clearly, the elements could be divided into eight group.

The first group has10 elements*, including Co, Sc, Ni, Bi*, *Li, As, Cs, Cu, Mn and Zn. Both Co* and *Ni* belong to ferrophilic elements, which generally exist in basic or ultrabasic rocks. Sc was a rare element and usually exists in alkaline rocks. *As* and *Bi* belong to sulfur philic elements and were closely related to underground thermal movement. Li belongs to alkali metal elements, and its source may be related to geothermal fluids according to relevant studies. Cu and Zn were sulfur philic elements, which mainly form sulfide in nature, and tend to be enriched in the hydrothermal stage after magmatic stage. Cs and Mn belong to oxygen philic elements, and *Cs* was an alkali metal element, which mainly occurs in the Earth's crust and was related to hydrothermal action. The second type was *Sb*, *Sn* and *W*, which were closely related to volcanic magmatic activity. The third type was Pb, which mainly exists in acidic magmatic rocks. The fourth type was *^{210}Po*, and its distribution was closely related to the thermal control structure. The fifth type was *Hg*, which was more active and volatile. Under the action of geological processes, atmospheric radiation and groundwater, it was easy to migrate and form regional enrichment phenomenon. The sixth type was the *Be* element, which was closely related to high temperature hydrothermal solution. The seventh type was *Rb* element, similar to *Be* element, which was closely related to high temperature hydrothermal solution.The eighth group was *Mo* element, which was closely related to volcanic and magmatic activities.

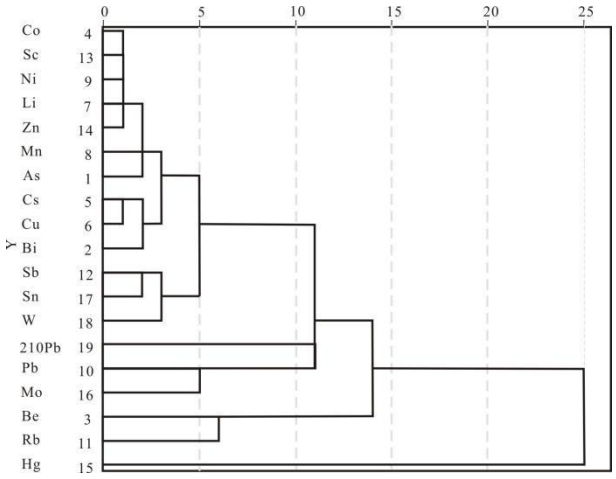

Figure 3 Pedigree of R-type cluster analysis of soil elements

3.2 Distribute characteristics of thermal elements

Result show a certain degree of spatial distribution regularity in the distribution. They was closely related to the fault location. In order to summarize the spatial distribution law and abnormal regional distribution characteristics more intuitively and systematically, the original data can be normalized by elements and then the mean value of sampling points can be obtained to obtain the superposition value of new elements.The normalization formula was as follows:

$$x' = \frac{x_i - x_{min}}{x_{max} - x_{min}} \quad (1)$$

Where, x' is the normalized processing result; x_i is the data point of i; x_{max} is the maximum value of the sample; x_{min} represents the minimum value of the sample.

The contour map of the elements after normalization and superposition processing shows all anomalous areas of soil elements in the study area(Fig 5). Comparing the two figures, it can be seen that the content of those elements in Daxing uplift in the north of the study area was significantly less than that in Niutuozhen uplift in the south. However, the abnormal values were not as obvious as the latter.The

distribution trend of contour lines of the element values shows that the anomaly distribution match well with the fault lines, which were mainly distributed in the following locations :(1)near the F1 Nanyuan -- Tongxian fault (the junction of Beijing sag and daxing Uplift), located in and around the town of quantou;(2) the border of Lirangdian Town and Xinlizhuang Town; (3)Along the Niudong fault of F10, near Mazhuang Towns-Nanmeng; (4) Niutuozhen - Longhu Village and its surrounding areas.There was no particularity in the abnormal areas in the other areas. The lower value areas were mainly distributed in large structures or located between faults, such as Lirangdian Township.

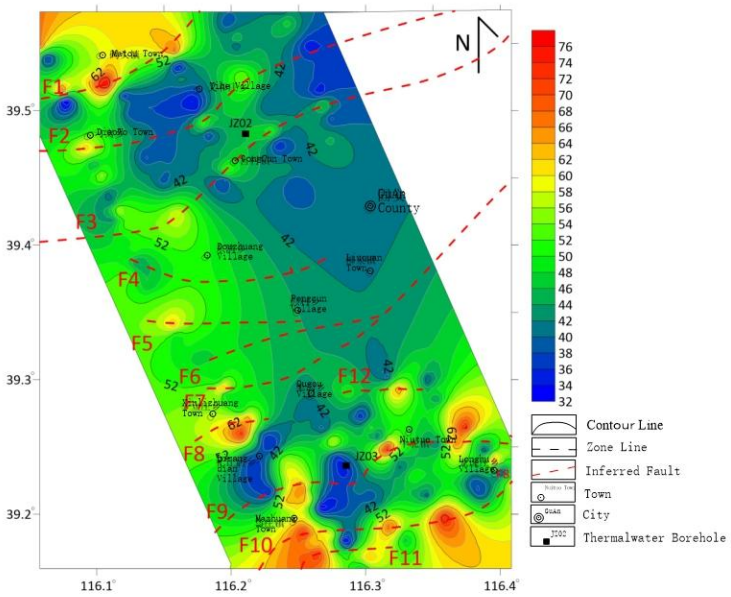

Figure 4 Contour map of thermal elements after normalized superposition processing in the study area

3.3 Profile anomaly characteristics of thermal elements

A typical geological profile of long section of thermal elements along Daxing Uplift-Baxian Sag shows in (Fig 6). The typical section GA01 runs through the north to the south of the study area in the geological structural units, including I Beijing Sag,II Daxing Uplift,III Langgu Sag, IV Niutuozhen Uplift and V Baxian Sag.

As can be seen from the figure, *Co, Sc, Ni, Bi, Li, As, Cs, Cu, Mn* and *Zn* elements have a similar trend. Moreover, the values of elements in Daxing Uplift and Niutaozhen Uplift was more obvious fluctuating than that in the depression area, in which the values in the depression area was lower. The distribution of element content has a certain relationship with the thickness of the cap layer. There were less variation of the value in the section with thick cover layer . Result shows that there a good distribution between the peak element content and the fracture location.The value of Sb, Sn and W elements was basically the same trend, that was, larger in the uplift area and smaller in the depression area. For example, III Langgu sag has certain similarity with the first type of elements. Except those in the Nanyuan-Tongxian fault (F1)..

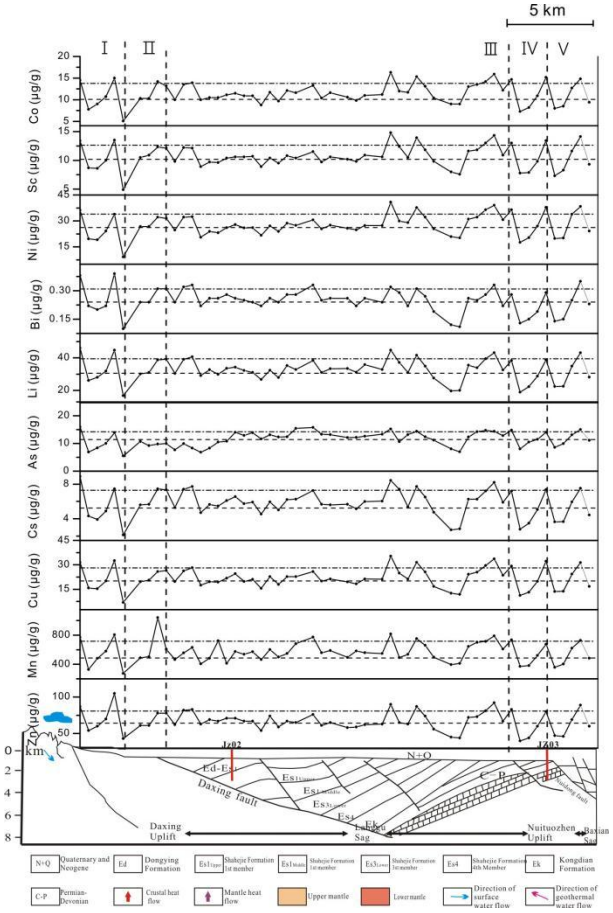

Figure.6: Cluster analysis of the first group of element profile and typical geological profile of Daxing Uplift-Baxian Sag

I Beijing sag； II Daxing Uplift；III Gulang Sag； IV Niutuozhen Uplift； V Baxian Sag

4 RADIOACTIVE GEOTHERMAL GEOTHERMAL GEOCHEMISTRY OF ROCKS

4. 1 Characteristics of thermal conductivity

Thermal conductivity of 101 samples from borehole JZ01 (a), JZ02 (b) and JZ03 (c) VS depth were plotted (Fig 75). As show in the figure , the average thermal conductivity of basalt and quartzite samples was 3.27g/cm3, ranging from 1.45 to 6.37g/cm3. This average value was generally higher than the average value of the lithosphere (2.85W/mK). The thermal conductivity values of clay, gravel, mudstone, basalt and quartzite was lower than the average value of the lithosphere , with average values of 2.07W/mK, 2.14W/mK, 2.35W/mK, 1.99W/mK and 2.92W/mK. .The lower thermal conductivity value of clay, sand and gravel, mud rock, basalt and the lower thinner quartzite layer indicated they have poor heat conduction abilities. The interbedded mudstone of the study area can keep the heat from escaping from the thermal reservior,, playing as the cap layer.The average thermal conductivity of dolomite and limestone was 5.92W/mK and 3.67W/mK, respectively, which was significantly higher than that of mudstone, conglomerate and gneiss. Among 8 limestone samples in borehole *JZ02*, 7 samples were greater than 4.5W/mK and 2 of them were greater than 5.0W/mK. These thermal conductivity was higher than the average of lithospheric (2.010W/mK). Among the dolomite samples of *JZ03* and *JZ02*, 7 samples were greater than 5.0W/mK, and 3 were greater than 6.0W/mK, and the highest value of was 6.634W/mK. These thermal conductivity values of the dolomite from the borehole were close to that of the rock mountain area, and much higher than the average value of the crustal rock (2.85W/mK). The average thermal conductivity of dolomite and limestone overlying conglomerate was 3.24W/mK, with a wide range from 1.99W/ mk-5.43 W/mK, which was obviously lower than the former playing a good thermal insulation. The thermal conductivity values of the two pebbled

sandstone samples in drill hole *JZ01* were greater than 5.0W/mK. The thermal conductivity of deep gneiss was 2.59W/mK on average and ranges from 2.10 to 3.24W/mK, which was slightly higher than that of mudstone.

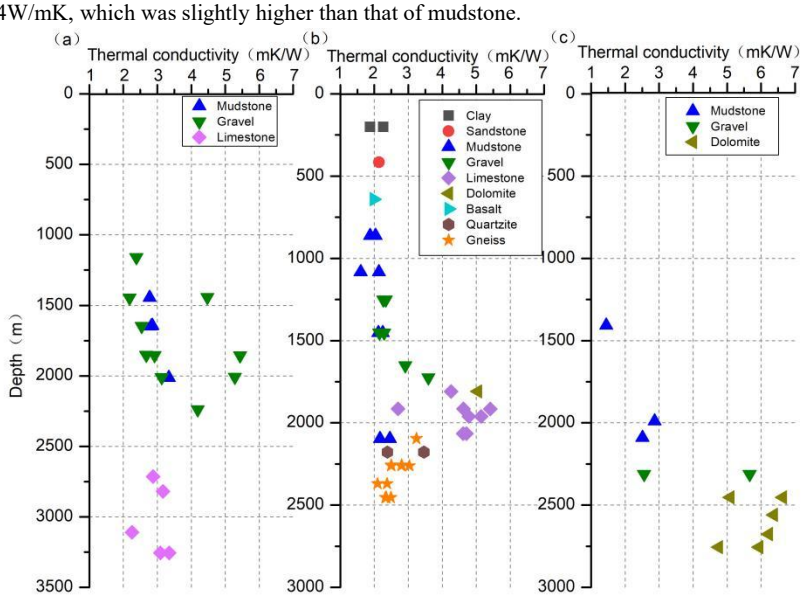

Figure5 Thermal conductivity VS depth of borehole JZ01 (a), JZ02 (B) and JZ03 (c)

4.2 Characteristics of radioactive elements

The U in gravel, mudstone, conglomerate, quartzite and limestone of *JZ01* were higher than those of the other two boreholes, with an average value of 1.29μg/g, 1.71μg/g, 1.41μg/g, 1.99μg/g and 1.37μg/g, respectively. These values were higher than the crustal abundance of North China platform,1.0μg/g. U in basalt, gneiss, dolomite and limestone of *JZ02* were less abundant, with mean of 0.12μg/g, 0.52μg/g, 0.40μg/g and 0.78μg/g, respectively. There values were , however, lower than 1.0μg/g.

Th was also analyzed in quartzite and gneiss, with an average value of 14.74μg/g and 11.40μg/g respectively. Meanwhile, of gneiss rock, the maximum value can reach 53.88μg/g of JZ01. The mean values of Th in these three boreholes were 5.29μg/g, 7.63μg/g, 9.62μg/g, 5.87μg/g and 8.20 μg/g, respectively. They were higher than the value of the crustal abundance of the North China platform(5.0μg/g). Th in dolomite, basalt and limestone of *JZ02* were less abundant.The mean values were 0.83μg/g, 0.83μg/g and 3.57μg/g, respectively,all smaller than 5.0μg/g .

There radioactive elements were analyzed as show in Fig 6 with Th/U VS depth of JZ01, JZ02 and JZ03 boreholes.

Th/U can be used to indicate the change of heat generation rate with depth. The average *Th/U* of JZ01, JZ02 and JZ03 were 5.29, 10.16 and 4.02, respectively. Only the *Th/U* of JZ03 was slightly lower than the world average level (4.7-5.0)[10] . Expectation the sample of gneiss from JZ02, *Th/U* of dolomite and limestone were generally lower, while that of mudstone and conglomerate were higher and gradually decreases

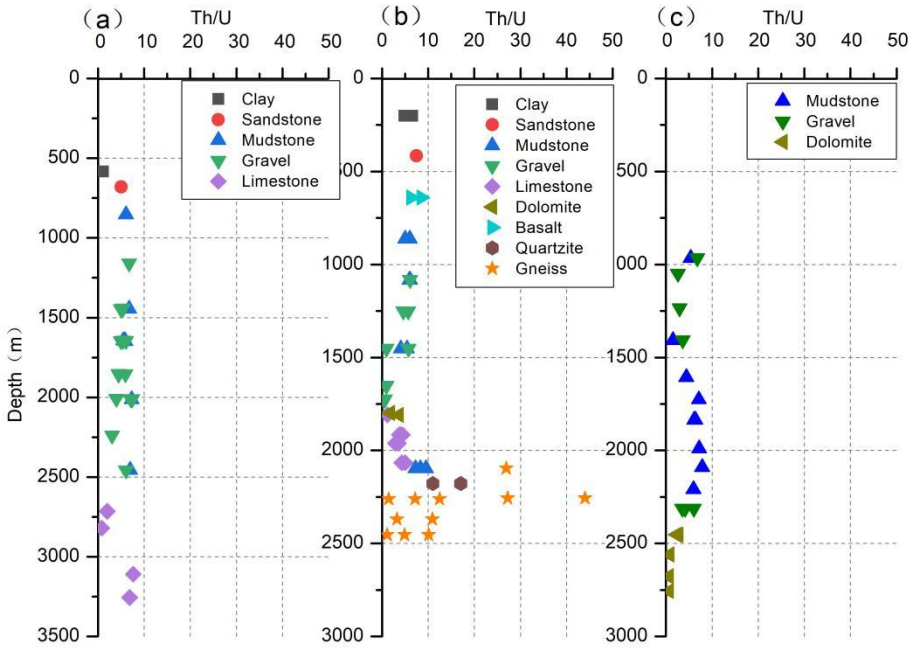

Figure 6 Th/U VS depth in boreholes JZ01 (a), JZ02 (b) and JZ03 (c)

4.3 Characteristics of radiogenic heat flux

The radiogenic heat flux can be caculated by U, K and Th element, usually obtained by gamma ray logging[11]. The formula proposed by Rybach(1967)[12] was the most commonly used to calculated radiogenic heat flux from the cust.

$$A = 10^{-2}\rho(9.52C_U + 2.56C_{Th} + 3.48C_K) \quad (2)$$

Where, A was the radiogenic heat flux of rock, $\mu W \cdot m^{-3}$; ρ was the rock density, $g \cdot cm^{-3}$; C_U, C_{Th}, C_K were the contents of radioactive thermogenic elements uranium, thorium and potassium respectively, μg/g.

The variation of radiogenic heat flux of rocks VS depth was shown in Fig 7. Results show that limestone and dolomite have low radiogenic heat flux. The average values were 0.75 μW/m3 and 0.19 $\mu W/m^3$ for limestome and dolomite. Radiogenic heat flux were ranging from 0.06 -1.49 μW/m3 and 0.06-0.72 $\mu W/m^3$, respectively. These consisted with the previous studies that the North China platform limestone was 0.29 $\mu W/m^3$ and dolomite was 0.25 $\mu W/m^3$ with lower radiogenic heat fluxs [13]. However, radiogenic heat flux of limestone in *JZ01* borehole was relatively higher radiogenic heat flux, with an average value of 1.04$\mu W/m^3$ and ranging from 0.13 to 2.75$\mu W/m^3$, which may be caused by petrogenesis or cementation. Basalt, clay, and gravel also have lower radiogenic heat flux.The mean values were 0.11μW/m3, 0.34μW/m3 and 0.68$\mu W/m^3$, respectively, and ranges from 1.12 to 2.29$\mu W/m^3$, from 0.16 to 0.53μW/m3 and 0.68$\mu W/m^3$.The radiogenic heat flux of gneiss and quartzite was relatively higher, the average values were 1.26$\mu W/m^3$, 1.71$\mu W/m^3$. They range from 0.39 to 4.68μW/m3, from 1.12 to 2.29$\mu W/m^3$. Radiogenic heat fluxs of some samples were relatively high. Among them, 4 samples were greater than 2.50$\mu W/m^3$, with the maximum value 4.68$\mu W/m^3$. However, the average value was still lower than that of gneiss worldwide (2.50μW/m^3)[14]. Considering (1)large thick dolomite (limestone) rock strata and metamorphic basement , (2) relatively deep burial depth,(3) relatively high metamorphic degree and (4)relatively low radiogenic heat flux, radiogenic heat flux could not be the main heat source in the study area.

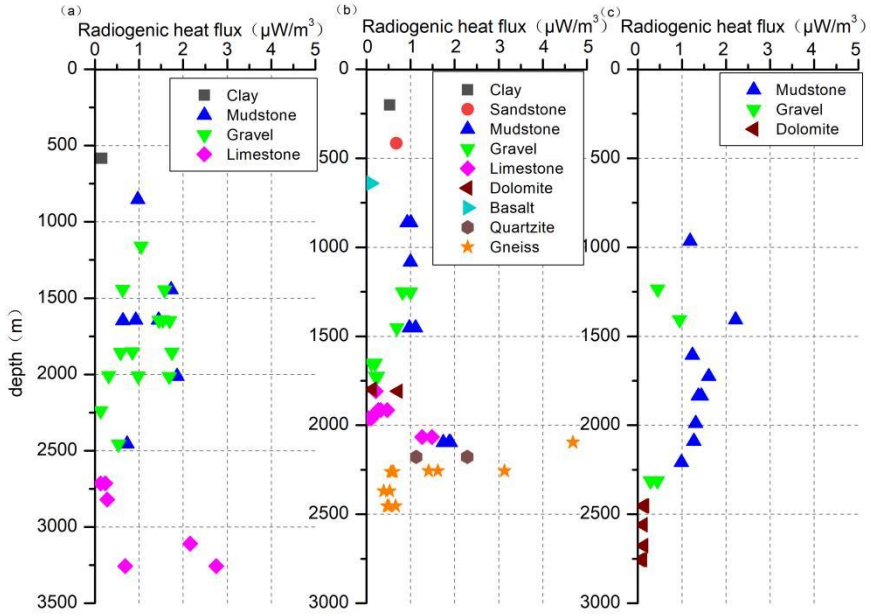

Figure 7 Radiogenic heat flux of borehole JZ01 (a), JZ02 (B) and JZ03 (c) with depth

5. GENETIC MODEL

Mantle heat flow in sedimentary basins can obtained by "Back stripping method" inversion[15]. The cacluting formula was as following with the parameter of terrestrial heat flow,radiogenic heat flux and crustal stratification thickness.

$$q_m = q_s - q_c = q_s - \sum A_i D_i \tag{3}$$

Where, q_c , q_m and q_s were crustal, mantle and surface heat flow respectively (mW/m^2) ; A_i was the radiogenic heat flux of layer i (μW/ m^3) ; D_i was the thickness of layer I. Comprehensive Cenogenic-Archean strata in these region was revealed by boreholes *JZ01, JZ02* and *JZ03* revealed . These boreholes were located in the north of Daxing Uplift, the south of Daxing Uplift and Niutuozhen geothermal field, respectively. The mantle heat flow in the northern Daxing Uplift area, the southern Daxing Uplift area and the Niutuozhen geothermal field were calculated 31.10mW/m^2, 27.26mW/m^2 and 41.33mW/m^2, respectively (Fig.8). Only the Niutuozhen geothermal field was higher than the average mantle heat flow , 32mW/m^2 , in Jizhong Depression [16]. However, it was still lower than the Cenozoic technically active areas or orogenic belts in China. For example, those , radiogenic heat fluxs, in the Inner Mongolian-Jihei orogenic belt in the northern North China Basin, Songnen block, the Qinling orogenic belt and Yangzi block range from 57 to 67mW/m^2 [17-18] , which values were close to that of the young terrane area (20-40mW/m^2)[19]. Our calculation indicated that the contributions of crustal radiogenic were 44.75%, 48.37% and 36.91% to the total heat flow. They were all less than 50%, even the global average (54%) [17]. This means that lithosphere thermal structure of this region was the typical "hot mantle and cold crust". That was, the destruction of the eastern North China Craton caused significant thinning of the lithosphere and crust and the uplift of Moho surface. This result in driving the deep mantle heat to the shallow, forming a "hot mantle cold crust" . While, because the thermal conductivity of rock strata in depression-uplift area was different, heat would be concentrated in uplift area or buried hill zone. The groundwater was mixing water with atmospheric precipitation and paleo-precipitation in Taihang Mountains at a slow migration rate. The deep bedrock lithology was mainly distributed with dolomite and limestone which thermal conductivity was high. Therefore, heat from the mantle easily continuously flow through into these rock by conduction. Under the action of dissolution of water for many years, fractures were developed to contain more thermal water. The overlying sand-mudstone with low thermal conductivity can keep the heat from escaping. Nevertheless, big faults, such as Niudong fault, always played role as heat or water flowing channel. Hydrological head from the mountain,the high attitude, drive them upwell and release from deep circulation.

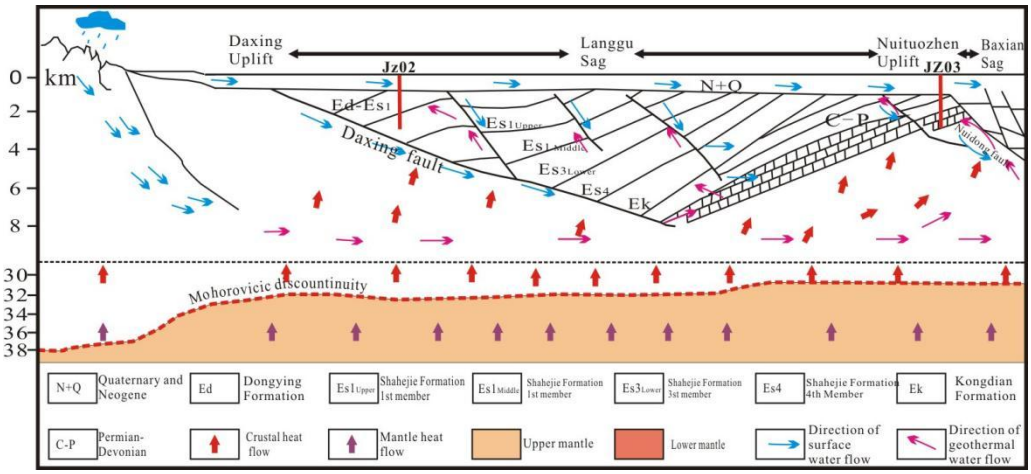

Figure 8 Geothermal genesis model in the study area

6 CONCLUSION

Soil elements, such as *As, Bi, Sb, Hg, Be, As, Li, Cu, Zn, Mn, Co, Cs, Sc, Ni, Pb, Rb, Sn, Mo* and *W*, were obviously correlated with each other. They were enriched to a certain extent in some areas. In our study area, these elements from the Niutuozhen rise in the southern part of the study area were higher than those from the Daxing uplift. Their distribution has a good relationship with the distribution of deep faults such as Daxing Fault and Niudong Fault. High 210Po in soil and radon in hot water were both found in the southern Niutuozhen . This suggests that these elements in the soil were related to the deep hydrothermal fluid flowing upward along the deep and large fault.

The study of rock properties shows that the thermal conductivity of limestone and dolomite were 3.92W/mK and 5.75W/mK, respectively, which were higher than those of other types of rocks. However, the radiogenic heat flux of these two rocks was low in the study area. These results indicated that these two types of rocks were conducive to conducting heat flow from deep and make good contributions to thermal reservoir. The overburden was mudstone and conglomerate with large thickness, good water permeability and low thermal conductivity. These properties help to store heat in thermal reservoirs. The thermal conductivity of deep gneiss was 2.59W/mK on average, which was lower than that of other rocks. However, the radiogenic heat flux of this rock was 1.26μW/m^3 on average, which was higher than that of other rocks in this area.

Based on the radio-geochemical characteristics, the heat flow from the crust was calculated from 36.9% to 48.4%, while the heat flow from the mantle was less than 50%.This indicated that the lithography thermal structure in these areas was "hot mantle and cold crust". The heat mainly comes from the mantle by heat conduction.

[1] Van der zwaan Bob-Dalla-Longa-Francesco. Integrated assessment projections for global geothermal energy use[J]. Geothermics, 2019, 82: 203-211.

[2] Lin Wenjing, Liu Zhiming, Wang Wanli.Geothermal resources and potential assessment in China [J]. Geology in China, 2013, 40(1): 312-321.

[3] Wang Guiling, Liu Yanguang, Zhu xi. Current situation and development trend of geothermal resources in China [J]. Earth science frontiers, 2020, 27(1): 1-9.

[4] Zheng Liying. Distribution characteristics and resource evaluation of Cenozoic geothermal reservoir in the Beijing-Tianjin-Hebei region[D]. China University of Geosciences (Beijing), 2015.

[5] Zhang Dezhong, Liu Zhigang, Lu Hongliu. The title of the book is missing[M]. Geological Publishing House, 2013.

[6] Liang Hongbin, Qian Zheng, Xin Shouliang. Evaluation and exploitation of geothermal resources in Jizhong Depression [J]. China petroleum exploration, 2010, 15(5): 63-68, 86.

[7]Wang Guiling, Zhang Wei, Lin Wenjing.Study on geothermal resource accumulation model and potential in Beijing-Tianjin-Hebei region [J].Geology of China, 2017, 44(6): 1074- 1085.

[8] Chen Moxiang. The title of the book is missing [M]. Beijing: Geological Publishing House, 1988.

[9] Du Jinhu. The title of the book is missing [M].Beijing: Science Press, 2002.

[10] Brian F. Windley. The continental crust: its composition and evolution[J]. Physics of the Earth and Planetary Interiors, 1986, 42(3): 196- 197.

[11] Luo Xin, Zhu Chuanqing, Zhang Baoshou. Estimation of sedimentary heat generation rate in Tarim Basin by natural gamma logging [J]. Journal of Geology, 2020, 94(7):2078-2088.

[12] Ladislaus Rybach. Radioactive heat production in rocks and its relation to other petrophysical parameters[J]. Pure and Applied Geophysics Pageoph, 1976, 114(2): 309-317.

[13] Chi Qinghua, Yan Mingcai. Radioactive elements in rocks of the North China Platform and thermal structure and temperature distribution of modern continental lithosphere [J].Chinese Journal of geophysics, 1998, (1): 38-48.

[14] I. M. Thybo H. Jakobsen K. Sorensen N. K. Nielsen L. S. K. Artemieva. Heat production in granitic rocks: Global analysis based on a new data compilation[J]. Earth-science Reviews, 2017, 172: 1-26.

[15] Wang Jian,Wang Jiyang,Xiong Liangping. The title of the book is missing [M].Beijing: Science Press,1992.

[16] Qiu Nansheng,Hu Shengbiao,He Lijuan. The title of the book is missing [M].Qingdao: China University of Petroleum Press, 2019.

[17] Gao Shan, Zhang Benren. Radioactivity of rocks and modern thermal structure and thermal state of lithosphere in Qinling Orogenic belt and its adjacent areas [J]. geochemistry, 1993, (3): 241-251.

[18] Li Shuanglin. Radioactive elements and thermal structure and temperature distribution of lithosphere in the Manzhouli-Suifenhe Geoscience Section, China [J]. geological-geochemical characteristics, 1996, (2): 73-77.

[19] A Vladimir,M Podhradska,M Kulikova,et. Comparison of therapeutic results of clinical II laryngeal carcinoma treated with various methods and concurrent monitoring changes in cellular and humoral protection[J]. Otorinolaryngologie a Foniatrie, 1989.